Scientific Research Publishing

Open Journal of Applied Sciences, 2023, 13, 1145-1162
https://www.scirp.org/journal/ojapps
ISSN Online: 2165-3925
ISSN Print: 2165-3917

Effect of High-Speed Solar Winds Turbulence Upstream of the Earth's Magnetosphere: Case of the Outer Minima of Solar Cycles 20, 21, 22, 23 and 24

Inza Gnanou[1,2*], Salfo Kabore[2], Aristide Marie Frédéric Gyebre[2], Christian Zoundi[2], Jean-Louis Zerbo[2,3], Frédéric Ouattara[2]

[1]École Normale Supérieure, Koudougou, Burkina Faso
[2]Department of Physics, Laboratoire de Recherche en Énergétique et Météorologie de l'Espace (LAREME), Université Norbert ZONGO, Koudougou, Burkina Faso
[3]Department of Physics, Laboratoire de Matériaux, d'Héliophysique et Environnement (LaMHE), Université Nazi BONI, Bobo-Dioulasso, Burkina Faso
Email: *gnanouinza@gmail.com

How to cite this paper: Gnanou, I., Kabore, S., Gyebre, A.M.F., Zoundi, C., Zerbo, J.-L. and Ouattara, F. (2023) Effect of High-Speed Solar Winds Turbulence Upstream of the Earth's Magnetosphere: Case of the Outer Minima of Solar Cycles 20, 21, 22, 23 and 24. *Open Journal of Applied Sciences*, **13**, 1145-1162.
https://doi.org/10.4236/ojapps.2023.137091

Received: June 21, 2023
Accepted: July 24, 2023
Published: July 27, 2023

Abstract

Highly turbulent environment, the solar wind is a stream of very energetic particles mainly made of protons and electrons. During its trip in the interplanetary space, this solar flow becomes more accelerated during the outer minima (descending phases) of the solar cycles and can therefore influence all of humanity and its technology. These disturbances lead to socio-economic consequences requiring a precise knowledge of the climate variability. Using a statistical approach, we evaluate the response of the Earth's magnetosphere to the High-Speed Solar Winds (HSSW) forcing during the peaks of the last five outer minima. To do so, 1UA data of solar wind and magnetic field parameters were extracted from OMNI browser. Analysis of the energetic solar plasma particles shows that strong geomagnetic field variations can occur even in the absence of large solar disturbances. While the normalized reconnection rate was estimated to be ~21% of the total variance of the magnetospheric variables, the upstream of the magnetic cavity was perturbed 80% of the time with large energies recorded. As a result, Earth's magnetosphere becomes denser (*i.e.*, more drag), which is a problem for spacecraft. Thus, the coupled solar wind-magnetosphere system follows scale-invariant dynamics and is in a state far from equilibrium. Our analysis provides insight into the main cause of geomagnetic storms with more than 97% of HSSW imposed in the range 300 - 850 km/s. These high-speeds lead to auroras that can disrupt electrical and communication systems.

Keywords

Solar Wind, Outer Minimum, Magnetosphere, Geomagnetic Field, Solar Disturbances

1. Introduction

The Sun, source of life providing heat, light and food with a central place in agriculture, continues to be nowadays, a source of questions for all humanity. From this source, solar events are continuously ejected into interplanetary space in the form of radiation (X-rays, UV, etc.) and energetic particles (solar wind jets, interplanetary coronal mass ejections ICMEs, etc.). Thanks to space missions such as Advanced Composition Explorer (ACE), WIND, Operating Missions as a Node on the Internet (OMNI), Parker Solar Probe (PSP), Magnetospheric Multiscale (MMS), the dynamics and properties of ICMEs have been studied using in situ data at 1 AU. These studies, while showing the impact of these flares on space weather as well as their implication in solar-terrestrial physics, advance our knowledge which will be very important for future space missions. It is well known that ICMEs cross and interact with the solar wind in the background. However, the nature of this interaction depends on the structure of the plasma, the solar wind and the generally faster ICMEs. The proof of the solar wind/ICMEs interaction and of two varieties of the solar flow (slow and High-Speed Solar Winds) has been one of the great triumphs of the space age, and much has been learned about their physical nature. Nevertheless, our current understanding of the structure of solar winds when their speed becomes sufficiently high is far from complete. We also do not understand the conditions of the closed to open magnetic topologies on the dayside of the Earth's magnetosphere under the effect of fluctuating HSSW. In general, our ideas about the structure of HSSW are still developing over average periods of 11 years since 1963. These ideas need to be tested with other periods of observations, for example, during the outer minimum of solar cycles to better elucidate the upstream forcing of HSSW particles.

Indeed, during the descending phase (outer minimum) of solar cycles, the solar wind becomes more accelerated. These sufficiently high speeds have an impact on planetary bodies, electronic components of spacecraft, electrical and navigation systems, energy variation of charged particles, geomagnetic storms, magnetospheric dynamics, etc. In addition, changes in the Earth's environment created by human activities can induce disturbances in local and even regional climatic characteristics. Electric and magnetic fields induced on ground by these solar-generated disturbances also have major influences on the operation and reliability of space and terrestrial systems/services (radio waves, communication systems, power and aviation grids, artificial satellites, etc.), or even threaten human health through carcinogenic diseases, depression, heart failure, immunological modifications [1] [2] [3] [4]. Above all, without a stable magnetic field to protect the Earth (magnetosphere), we would be incredibly vulnerable to solar storms. However, this magnetic bubble is neither rigid nor completely impermeable, and will in fact be under pressure from solar particles. Thus, a small portion of the solar wind penetrates this region on the night side. These particles are then concentrated in the plasma sheet from where they are accelerated towards the Earth to constitute harmful elements for humanity [5] [6]. In reality, different populations of solar wind particles are not independent. They communicate with each other thanks to a permanent large-scale circulation induced by the solar wind inside the magnetosphere. This circulation constancy is linked to an electric field dawn-dusk that can cause irregularities in the magnetosphere. Thus, all these disturbances have economic consequences whose cost can only be correctly evaluated by a precise knowledge of climate variability.

The challenge of predicting with precision and as quickly as possible, *i.e.* from solar observations and based on the knowledge of physical processes, requires expertise on all stages of the phenomena from Sun to Earth. In this scenario, interplanetary signatures are the key to advance towards the Earth and back towards the Sun to finally discover with precision, the geoeffectiveness of the upstream of the terrestrial magnetosphere. Objective of this manuscript is to contribute to a better knowledge of the dynamics and structure of the Earth's magnetosphere in the face of extreme fluctuations in solar activity during the outer minima of solar cycles 20 to 24. Note that solar cycle 25 (started in 2019), whose outer minimum is scheduled for 2029 according to NASA, would not be taken into account in this study. Given the complexity of the magnetospheric system, our study will use a statistical approach rather than a univocal study. In this case, there is evidence for a statistical relationship between HSSW turbulence and geomagnetic response, although it cannot be considered the only physical mechanism involved in the dynamics of the magnetosphere. More clearly, in an electric current approach, this work, which is a continuation of [7], conducts a statistical analysis of HSSW populations during the last five outer minima. The main reason for studying HSSW is that they are a potential hazard to the entire Earth and to space systems. First, this paper introduces data set and methodology adopted in Section 2. Then, Section 3 describes our results and various interpretations. Finally, a conclusion is presented in Section 4.

2. Data and Methodology

In this article, various one-hour rate space datasets (averaged if necessary), available in the OMNI "https://omniweb.gsfc.nasa.gov/ow.html" and ISGI "https://isgi.unistra.fr/data_download.php" public domains, have been used to obtain information relating to Solar Wind (SW) and interplanetary magnetic field (IMF) parameters. The data set required to analyze a solar wind population in this article has been carefully examined to identify HSSW currents and ICMEs. Only cases where the B_y [nT] and B_z [nT] components of the IMF, the

SW velocity V_x [km/s], the frozen or zonal electric field E_y [mV/m] and the geomagnetic index A_a [nT] were available simultaneously in geocentric coordinates of the GSM solar magnetosphere were considered in this study.

Furthermore, to determine the high-latitude structure of the E_M electric field [mV/m] controlling SW particle circulation in Earth's magnetosphere, the field transformation law [8] [9] was used, neglecting Earth-related corotation. This law is defined by Equation (1):

$$E_M = 0.13E_y + 0.09 \quad (1)$$

where E_y [mV/m] represents the zonal electric field.

In addition to the magnetospheric trapping and energization highlighted by [10], the coupling function developed by [11] was used to quantify the rate of magnetic reconnection on the dayside of the magnetosphere. This coupling function is represented by Equation (2) defined by:

$$\Phi_D = \Lambda V_x^{4/3} B_{yz} \sin^{9/2}\left(\frac{\theta}{2}\right) \quad (2)$$

where $\Lambda = 3.3 \times 10^5\ m^{2/3} \cdot s^{1/3}$, V_x is the speed of the solar wind [km/s], B_{yz} is the transverse component of the IMF [nT] and θ, the clock-angle, *i.e.* the angle between IMF vector projected into GSM Y-Z plane and Z axis in degree.

In this manuscript, value of the dayside reconnection rate noted Φ_D [Wb/s], was normalized to its average value $\langle \Phi_D \rangle$ of the entire analysis period. This normalized rate would be denoted $\Phi_D / \langle \Phi_D \rangle$. This normalization was chosen to allow the magnetospheric system to accommodate the upstream forcing of energetic HSSW particles.

3. Discussion of Results

3.1. Solar Flux Structure and Magnetospheric Activities

The evolution of the statistical mean of solar wind speeds on an annual scale has been studied in this section. Figure 1 informs us that over the period 1964-2019

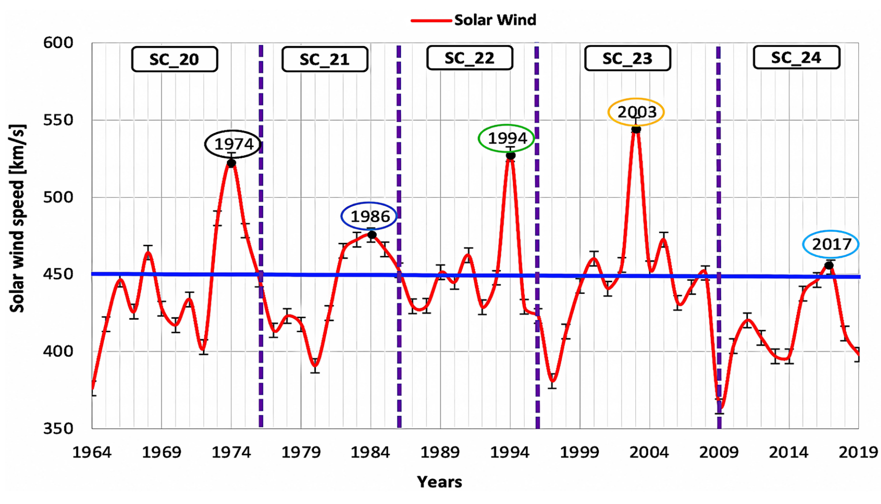

Figure 1. Annual change in average solar wind speed from 1964 to 2019.

covering the last five complete solar cycles (solar cycle 20 to 24), only about 34% of the years were under the influence of solar wind currents with annual speeds above 450 km/s (see upper part of the blue plot in **Figure 1**).

Out of 56 years in the selected period, five peaks (1974, 1986, 1994, 2003 and 2017) were recorded at the end of the solar cycle. These peaks belong to the outer minima of solar cycles 20, 21, 22, 23 and 24, respectively. Part of these results is corroborated by various scientific publications [12] [13] [14]. High velocities at the end of the solar cycle SC, characteristic of the High-Speed Solar Winds HSSW, originate from coronal holes CHs and trigger intense geomagnetic activities [15] [16]. On the one hand, one of the possible explanations is that HSSW originating from CHs, predominate in the descending phases of solar cycles [17] [18]. On the other hand, [19] also studied the fluxes produced by coronal holes (CH_HSSW) and those produced by solar flares (FG_HSSW). The latter authors revealed that CH_HSSW prevails during the decreasing phases of SC because large CHs extend toward the equator in these solar phases while the variation of FG_HSSW follows the 11-year sunspot cycle. Among the peaks of the five outer minima, the weakest are those of 1986 and 2017, in SC_21 and SC_24, respectively. Magnetic field strength was larger (0.65 nT and 0.60 nT, respectively) for the 1986 and 2017 peaks. From these findings, one can suggest that the low amplitudes of the 1986 and 2017 peaks of the outer minima of SC_21 and SC_24 are due to the large number of sunspots. However, during the outer minimum of SC_23 (year 2003), largest peak (546.80 km/s) is observed in the longest cycle of the solar cycles studied. A good part of these results is corroborated by the works of [15] [20] and [21].

In order to examine the structure of fast winds and topology of the solar magnetic field of the five observed outer minima, pixel diagrams or color diagrams [22] [23] relating to the daily averages of solar wind speeds (cf. panels (a) to (e) of **Figure 2**) have been constructed. As a reminder, pixel diagram is a diagram that gives an overview of the geo-efficiency of solar events. In this manuscript, this color-coded diagram, is constructed using daily mean solar wind speeds so that time flows from left to right in each row, then from top row to bottom row. On the panels in **Figure 3**, all the framed cells except the blue-white one, represent the recurrent days, *i.e.*, the main class of HSSW events (cf. panel (e) of **Figure 2**). The cells marked with the symbols "####" inform us of the absence of reliable data. And finally, the circled/hidden cells show the days of shocks (ICMEs). Thus, examination of the panels reveals that the year 1986 had many holes (unreliable data) and fewer HSSW (orange-red-green-yellow) compared to the other outer minima. However, year 2003 recorded more than 76% of solar flux reaching a peak speed of 450 km/s in the longest solar cycle (SC_23), or a little more than 12.5 years. Of the outer minima studied, highest annual average recorded in 2003 was only about 20% higher than lowest annual average (454.62 km/s) recorded during 2017. The high annual averages from the peak to the trough of the outer minima are due to both an increase in the relative frequency of very high velocities (greater than 450 km/s) and a decrease in the

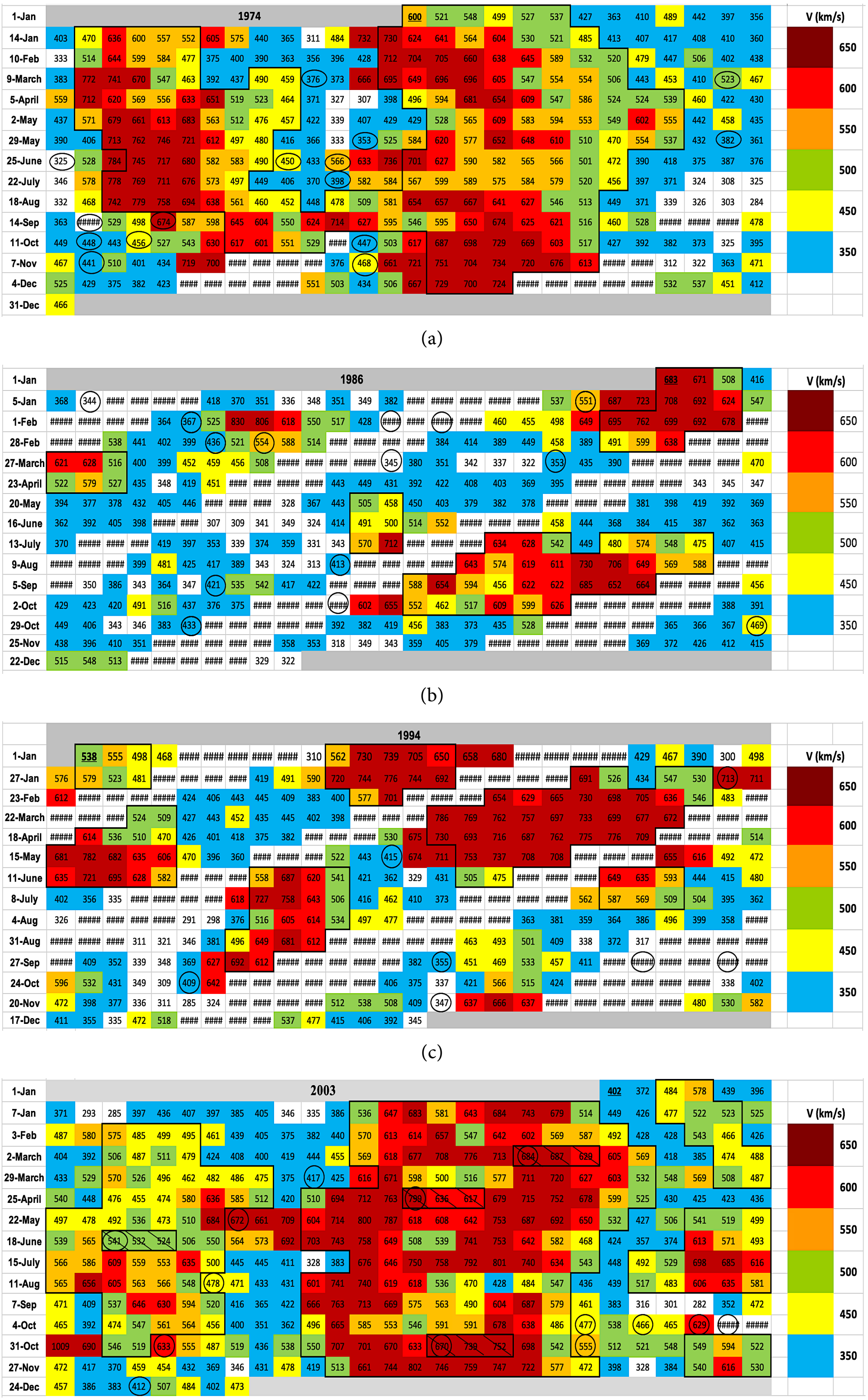

(a)

(b)

(c)

(d)

Current class

1-Jan	2017					511	404	434	461	601	691	686	675	647	570	487	396	365	368	334	317	311	474	592	546	499	508
23-Jan	439	348	341	419	586	520	438	440	626	681	663	627	566	579	562	505	456	419	419	396	347	329	313	307	366	481	512
19-Feb	556	503	430	405	471	599	512	419	369	397	509	685	680	655	620	604	576	533	520	467	391	392	340	332	351	376	345
18-March	321	315	315	496	642	609	552	476	387	531	673	642	625	670	584	488	420	419	412	470	422	531	486	427	435	438	394
14-April	399	334	340	312	321	408	553	552	690	723	672	593	524	462	404	378	372	378	410	379	344	382	344	349	368	367	364
11-May	373	387	320	321	431	568	488	405	457	655	631	545	508	449	373	323	326	360	360	483	399	361	373	398	425	369	350
7-June	336	308	315	290	329	445	496	469	411	477	479	561	475	376	336	330	336	375	439	516	465	425	408	346	373	449	419
4-July	357	317	336	387	335	461	558	583	480	395	359	327	449	520	541	431	406	614	569	586	635	586	580	455	436	407	361
31-July	339	378	391	373	567	667	613	500	432	404	393	403	550	573	475	401	378	481	573	672	696	585	554	467	404	348	340
27-Aug	336	294	330	363	529	602	584	506	492	529	446	526	740	585	498	593	499	459	438	664	676	644	617	512	459	413	361
23-Sept	361	336	367	320	486	654	592	502	461	427	403	365	384	422	398	412	362	323	414	513	579	668	595	543	460	379	392
20-Oct	420	389	413	375	437	592	542	445	380	341	307	284	292	348	396	406	364	315	444	609	540	632	547	457	388	383	401
16-Nov	479	424	397	367	359	551	502	415	371	382	318	387	432	396	458	460	403	340	329	506	540	500	433	373	332	402	469
13-Dec	446	400	352	342	511	603	522	434	380	328	346	468	486	448	430	389	366	372	358								

V (km/s)
650
600
550
500
450
350

(e)

Figure 2. Pixel diagrams of 1974 (panel a), 1986 (panel b), 1994 (panel c), 2003 (panel d) and 2017 (panel e) peaks.

relative frequency of low velocities (less than 450 km/s) daily. From these observations, peak of 2003 presents the frequent occurrence of high-speed solar wind currents with a peak of 858 km/s recorded on June 03, 2003 at about 7:00 pm UT. These findings are corroborated by [20] and [24].

High-speed solar winds propagate at very remarkable speeds ($V_{sw} \geq 450$ km/s on average daily over at least two solar rotations) and cause storms that are gradually triggered [25]-[30]. Placing ourselves in the context of geomagnetic activity and especially its new extension defined by [13] and then [23], we study the solar flux distribution on the set of selected outer minima, see **Figure 3**. Indeed, examination of panels (a), (b), (c), (d) and (e) of **Figure 3** show respectively that at least 98%, 98%, 99%, 96% and 96% of solar flux emitted by the Sun, has been under the influence of HSSW. From this analysis, it is therefore clear that at solar minimum, high-speed solar flux is the main contributor at 97% to the solar averages of the solar winds during outer minima. Analysis of all panels shows that more than 99% of the solar flux velocities are imposed in 300 - 850 km/s range, which range is corroborated by several authors [31] [32] [33]. Thus, we can suggest that the peaks of the outer minimum of SC remain the most extreme and magnetically disturbed periods.

Despite the smaller changes in HSSW from one outer minimum to next, overall, the mean velocity variations are nearly similar. Indeed, outer minima from SC_20 to SC_24 show significant HSSW contributions in the range 96% to 99%. This contribution is in very good agreement with [13] [22] and [34] [35] [36] in which, velocity limit of HSSW is set to characterize recurrent solar flux. Our analysis shows us to what extent, velocity distributions of the material flux are not all similar for the considered outer minima, whatever solar flux variation. In fact, velocity of solar flux changes due to acceleration/deceleration processes during its propagation in the interplanetary space. The important point is that Sun progresses in its activity [16]. During solar maximum and outer minimum of SC, likely sources of solar disturbances that can induce fluctuations in power grids and/or GPS signal transmission at ground level are ICMEs and high-speed flux [35]. Variations in the location of the solar wind source and the interaction

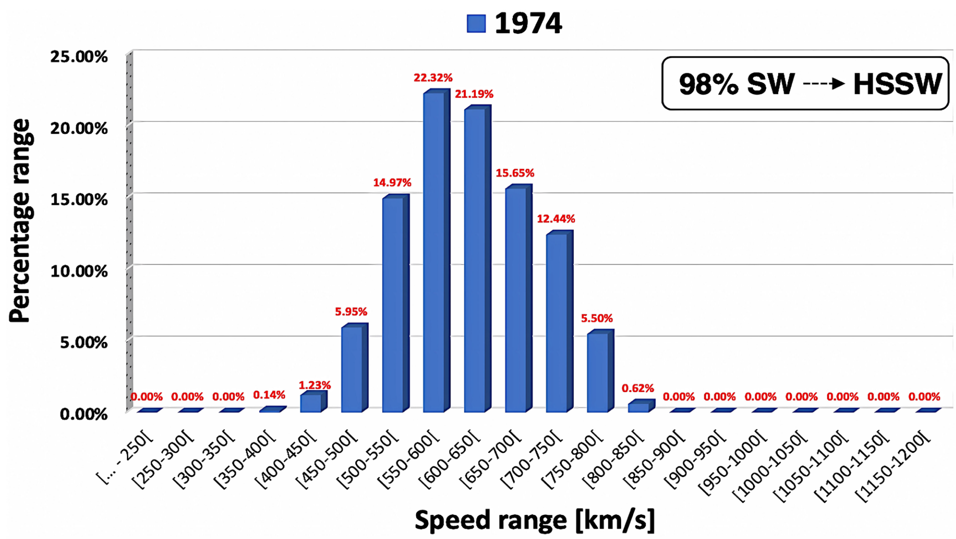
1974
98% SW ---> HSSW
Percentage range
25.00%
20.00%
15.00%
10.00%
5.00%
0.00%
0.00% 0.00% 0.00% 0.14% 1.23% 5.95% 14.97% 22.32% 21.19% 15.65% 12.44% 5.50% 0.62% 0.00% 0.00% 0.00% 0.00% 0.00% 0.00% 0.00%
[... - 250[[250-300[[300-350[[350-400[[400-450[[450-500[[500-550[[550-600[[600-650[[650-700[[700-750[[750-800[[800-850[[850-900[[900-950[[950-1000[[1000-1050[[1050-1100[[1100-1150[[1150-1200[
Speed range [km/s]

(a)

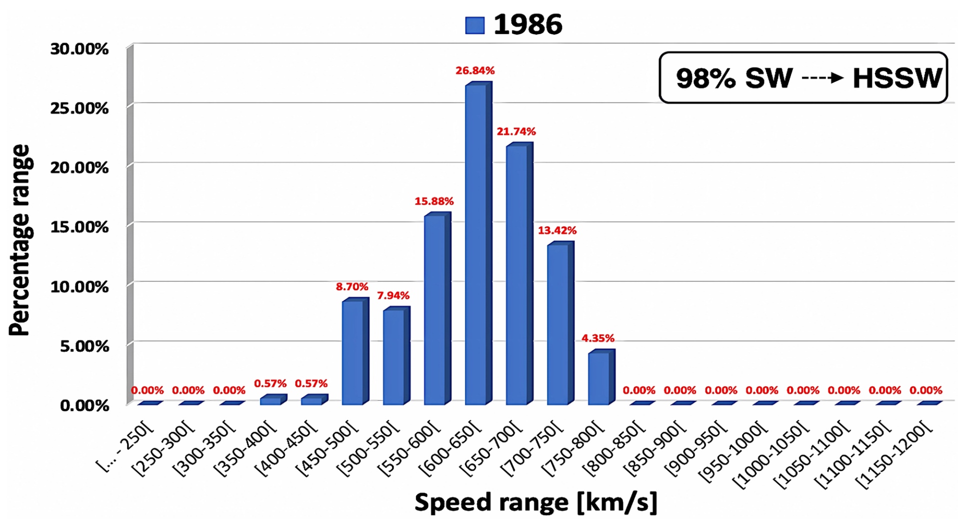
1986
98% SW ---> HSSW
Percentage range
30.00%
25.00%
20.00%
15.00%
10.00%
5.00%
0.00%
0.00% 0.00% 0.00% 0.57% 0.57% 8.70% 7.94% 15.88% 26.84% 21.74% 13.42% 4.35% 0.00% 0.00% 0.00% 0.00% 0.00% 0.00% 0.00% 0.00%
[... - 250[[250-300[[300-350[[350-400[[400-450[[450-500[[500-550[[550-600[[600-650[[650-700[[700-750[[750-800[[800-850[[850-900[[900-950[[950-1000[[1000-1050[[1050-1100[[1100-1150[[1150-1200[
Speed range [km/s]

(b)

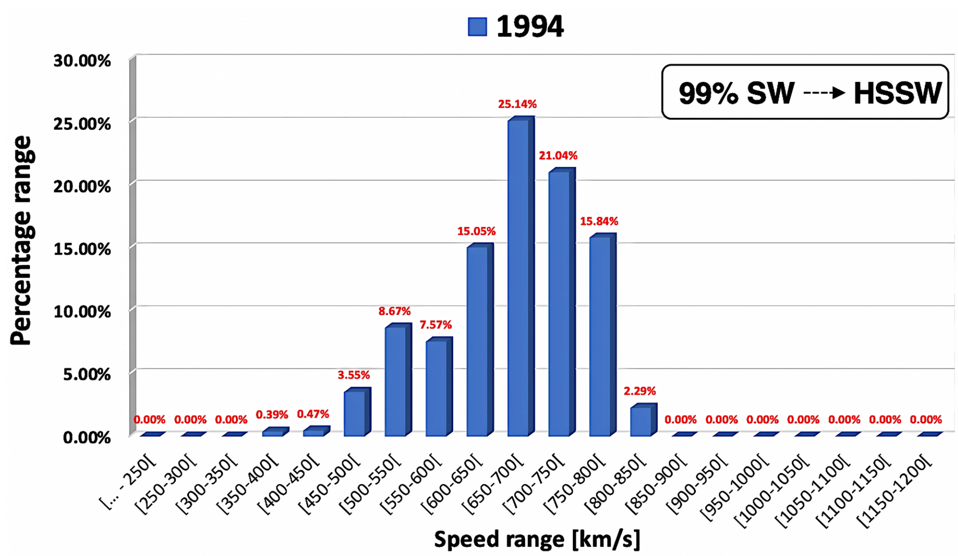
1994
99% SW ---> HSSW
Percentage range
30.00%
25.00%
20.00%
15.00%
10.00%
5.00%
0.00%
0.00% 0.00% 0.00% 0.39% 0.47% 3.55% 8.67% 7.57% 15.05% 25.14% 21.04% 15.84% 2.29% 0.00% 0.00% 0.00% 0.00% 0.00% 0.00% 0.00%
[... - 250[[250-300[[300-350[[350-400[[400-450[[450-500[[500-550[[550-600[[600-650[[650-700[[700-750[[750-800[[800-850[[850-900[[900-950[[950-1000[[1000-1050[[1050-1100[[1100-1150[[1150-1200[
Speed range [km/s]

(c)

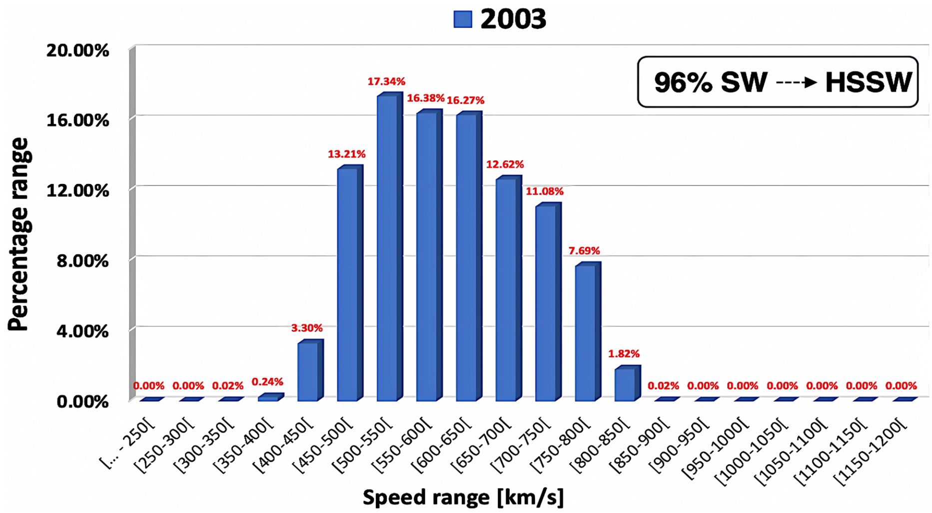

(d)

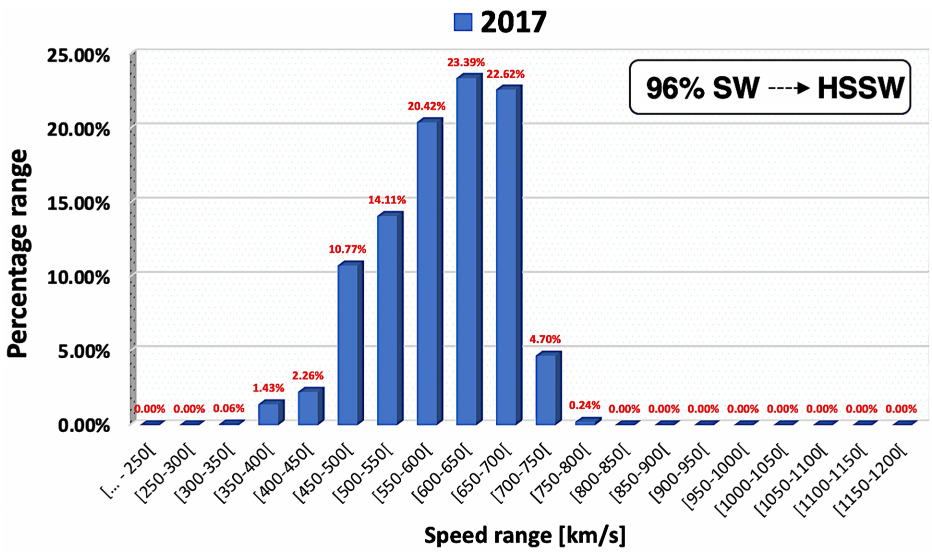

(e)

Figure 3. HSSW velocity distribution of 1974 (panel a), 1986 (panel b), 1994 (panel c), 2003 (panel d) and 2017 (panel e) outer minima.

of fast and slow solar winds produce changes in temperature and dynamic pressure (density and speed) of the solar wind.

Table 1 shows summary of ICMEs and HSSW studied in this manuscript, and reveals a striking disparity in values. Indeed, examination of this table shows that outer minima have recorded tens of interplanetary coronal mass ejections ICMEs emitted over durations of one to three days while the HSSW are of the order of 40 to 190 recorded events. Of the five selected outer minima, the peak of 2003 outer minimum recorded a higher number of recurring events. Given that recurrent activity represents the main class of HSSW events from CHs, co-rotating, with an apparent tendency to occur every 27 days (see pixel diagram in Figure 2), we suggest that magnetospheric activity was more important for 2003 peak of SC_23 outer minimum. This result is in perfect agreement with [7] and [13].

Table 1. Summary of solar events of outer minima.

	Outer Minima [year]				
	1974	1986	1994	2003	2017
Number of shocks	15	16	8	14	17
Number of recurring days	148	40	84	190	70
V_{sw} [km/s]	616.16	622.88	667.37	604.36	598.44
Dst [nT]	−16.31	−22.88	−32.70	−25.07	−19.96
A_a [nT]	37.27	33.03	45.42	41.12	34.06
B_y [nT]	−0.72	−1.15	−0.40	+0.12	+0.33
B_z	South	North	South	South	South

In general, statistical analysis of the solar flux particles shows different results according to the outer minima from SC_20 to SC_24. Indeed, Solar winds and terrestrial magnetosphere form a coupled system since the perturbations of the interplanetary medium are felt on Earth through magnetogram measurements [37]. As can be seen in **Table 1**, more than 80% of solar particles at the average velocity of about 622 km/s enter the Earth's magnetosphere with a south-pointing B_z ($B_z < 0$). From this study, it can be seen that solar wind particle velocity, geomagnetic index and intensity of the ring current growth rate |Dst| were at their optimum for 1994 peak. These quantities were so large that "bow shocks" could form whenever they are forced to circulate around the planets in the solar system. Such bow shocks will also form around spacecraft as they travel faster than the speed of sound through the atmosphere. [38] has shown that magnitude of solar wind turbulence upstream of Earth is strongly correlated with geomagnetic activity for a south-facing IMF-B_z. This increased turbulence upstream of the Earth, could cause greater convection in the Earth's magnetosphere; resulting in stronger current systems between magnetosphere and ionosphere. Our argument is in very good agreement with other subsequent studies on the role of solar wind fluctuations in geomagnetic activity during a south-pointing IMF [37] and [39]. From these findings, 1994 outer minimum was a year characterized by frequent occurrences of intense activity. This fact is corroborated by [20] [24].

However, over a wide range of magnetospheric activities, we find for all five outer minima, an almost linear increasing evolution of HSSW thrust and ring current (|Dst|) until 1994, followed by a depression over the outer minima rest. Contrary to the quantities elicited, when the dawn-dusk component (B_y) of IMF is negative, the geomagnetic activity and sunspot number often appear random for 80% of the time. While for positive B_y component (*i.e.*, for dusk), these same quantities decrease so that high velocities stabilized at 601.4 km/s on average towards the South, are observed at 03:00 pm UT over the remaining 20% of the time. [40] showed that the magnetospheric system remains in equilibrium if IMF-B_y component remains southward. [41] proved that magnetospheric convection intervals occur at 18% of the time. Our results are almost similar. However, the 2% discrepancy found between our studies could be due to the study intervals and/or the selected solar flux typology. This study suggests that magnetosphere and HSSW constitute a complex system in which several nonlinear subsystems coexist and are interconnected at many spatial and temporal scales. This argument is corroborated by various publications [42] [43] [44] [45] [46].

3.2. Geoeffectiveness of the Outer Minimum of Solar Cycles 20 - 24

Although there is a remarkable literature focusing on the geoeffectiveness (a relationship between the magnetosphere reaction and the system that impacts it) of large interplanetary disturbances more frequent during outer minimum of solar cycles, this study shows that significant geomagnetic activity is sometimes present even in the absence of such large disturbances. For example, for the peak of the 1994 outer minimum, A_a geomagnetic activity was at its peak (45.42 nT) while a smaller number of ICMEs (08 in total) were recorded. In this context and to understand perspective of this review, a distinctive feature of electric/magnetic fields and magnetic flux, drivers of the complex coupled solar wind-magnetosphere system, cannot be ignored. Indeed, geomagnetic response, although closely related to changes in the state of B_z component of the IMF (IMF-B_z), is also strongly affected by the intrinsic dynamics of the Earth's magnetosphere. [47] showed that dynamical state of the Earth's magnetosphere depends not only on HSSW, but also on the driving electric field. In addition, the effects of HSSW on the magnetospheric plasma have been studied in other works. As an illustration, it has been found that arrival of a low-density solar plasma at the leading edge of a HSSW induces a clear enhancement of magnetospheric convection [47] [48] [49] [50]. As can be seen in column 4 of **Table 2**, for an optimal E_M magnetospheric convection electric field (0.12 mV/m), solar flux density was lower (3.57 particles per cubic centimeter) and then significant for much lower E_M fields over the rest of the study period. However, peak of the 2017 outer minimum has a similar convective intensity but with a different average density. This difference could be related to the orientation of the east-west component of the IMF. Thus, during entire period of the selected outer minima, the Earth's magnetospheric cavity was stable only 20% of the time. This argument is corroborated by [51] and according to the scenario proposed by [52].

Table 2. Correlation and energy balance of outer minima.

	Outer Minima [year]				
	1974	1986	1994	2003	2017
E_M [mV/m]	0.09	0.04	0.12	0.10	0.12
n [cm^{-3}]	4.08	4.16	3.57	4.12	4.24
E_{in} [TW]	1.58	1.52	1.88	1.70	1.65
$\Phi_D / \langle \Phi_D \rangle$	18%	13%	30%	22%	20%
E_{in} & E_M	60%	76%	−59%	64%	56%
E_{in} & B_z	−59%	−74%	58%	−62%	−55%

Furthermore, analysis of cross-correlations between E_{in} & B_z and then between E_{in} & E_M shows very significant results for all outer minima. These positive correlations for E_{in} & E_M and negative correlations for E_{in} & B_z, are much more improved for a northern orientation of IMF-B_z. This suggests in this paper that particle trapping of HSSW in the Earth's magnetic cavity has a more enhanced influence on magnetospheric convection when IMF-B_z is pointed North ($B_z > 0$) for high intensity of IMF-B_y. This result is corroborated by [53]. The strong correlations are justified by the fact that no solar flux parameter can be dissociated from the interaction between HSSW and Earth's magnetosphere.

When comparing geoeffectiveness of the magnetosphere for different orientations of the IMF-B_y as performed in the previous paragraph, it would be more convenient to consider the similar diurnal forcing that is controlled by the IMF-B_z. Indeed, fluctuation of the IMF carried by HSSW affects daytime reconnection rate which causes fluctuations in the convective electric field of the magnetospheric system. Thus, for all state variables selected in this study, normalized reconnection rate remains more significant for the 1994 peak that had recorded large extreme solar activities. [54] studied the response of the magnetosphere to the forcing of HSSW. They showed that an enhanced daytime reconnection rate input to the magnetospheric cavity led to strong and frequent substorms. The frequency of occurrence of substorms would be higher for a southern orientation of the IMF-B_y according to [55]. Overall strength of solar events shown in **Table 2** demonstrates that strength of substorms was greater for the 1994 peak with a south-pointing IMF. For the set of outer minima according to said table, normalized reconnection rate accounts for about 13% to 30% of the total variance of magnetospheric variables. This suggests that the rate of magnetic flux conversion from a closed to an open topology on the dayside of the Earth's magnetosphere does not depend significantly on the HSSW number density, but rather on the frequent occurrences of intense solar activities and orientation of the IMF-B_z. Our results are in general agreement with measurements of the interpolar cap potential made by SuperDARN radar network on the one hand, and [11] on the other.

While it appears that dayside reconnection rate is controlled by the constantly changing conditions of solar flux upstream of the Earth's magnetosphere, however, when IMF-B_z is south-facing, the closed magnetic field lines are converted to an open topology by magnetic reconnection, which reconnection allows energetic HSSW particles to induce more intense geomagnetic activity. Thus, cavity controlled by the Earth's magnetic field entered different modes of response to the energy input from the interplanetary medium with an average of 1.64×10^{12} W per outer minimum. This fluctuation allowed internal parts of the Earth's magnetosphere to energize and trap important solar particles during outer minima (see **Table 2**). For example, magnetospheric cavity of the 1994 peak became very "inflated" due to a significant amount of accumulated energy of about 1.88×10^{12} W. The large energy observed, was manifested by frequent intense solar activities with an IMF-B_z antiparallel to the Earth's magnetic field (see last line of **Table 1**). The behavior of large energy injected into the upper atmosphere during HSSW impact, could have consequences on the chemistry of the atmosphere according to several authors [56] [57] [58]. Such consequences suggest that Earth's environment, and perhaps even the Sun, are sources of disruptions and failures in new technologies such as wireless communications and power systems on a local and geographical scale.

4. Conclusion

Based on a statistical approach rather than an individual study presented in Section 3 of this manuscript, we conclude that during the peaks of the outer minima, normalized daytime reconnection rate of the Earth's magnetosphere is likely to be enhanced when IMF-B_z is antiparallel to the geomagnetic field with sufficiently high solar flux currents. This rate fluctuates between 13% and 30% of the total variance of the selected magnetospheric variables. Although there is a magnetospheric response to large interplanetary disturbances as the interplanetary counterpart of HSSW, significant geomagnetic activity is sometimes present even in the absence of such large ICMEs. The asymmetry between HSSW and ICMEs makes terrestrial magnetosphere a complex non-linear system characterized by rapid transition processes. Therefore, HSSW represent stability criterion for the particularly loud areas of the outer minimum of solar cycles. Furthermore, we also discussed the contribution of the IMF-B_y component on the plasma circulation upstream of the magnetosphere. Our results show that for large IMF-B_y intensities with a north-pointing IMF-B_z, trapping and particle energization of HSSW in the Earth's magnetic cavity has an enhanced influence on the magnetospheric convective electric field. While it appears that HSSW cannot independently drive either their velocity, the orientation of North-South (B_z) and East-West (B_y) components of the IMF, or the electric field of the solar flux, we find it insufficient to elucidate our analysis alone in this paper. Thus, there are many fundamental unsolved problems in space physics, as we must begin the study of magnetospheric perturbations via HSSW turbulence with a focus on this "new" electric current approach that is still in a very rudimentary stage.

Acknowledgements

We are grateful to the OMNI Space Data Centers (http://omniweb.gsfc.nasa.gov/) for the availability of solar wind parameters. We also thank the ISGI center (http://isgi.unistra.fr/) for the geomagnetic index data.

Conflicts of Interest

The authors declare no conflicts of interest regarding the publication of this paper.

References

[1] Schwenn, R. (2006) Space Weather: The Solar Perspective. *Living Reviews in Solar Physics*, **3**, Article No. 2. https://doi.org/10.12942/lrsp-2006-2

[2] Hapgood, M., Angling, M.J., Attrill, G., Bisi, M., Cannon, P.S., Dyer, C., Eastwood, P., Elvidge, S., Gibbs, M., Harrison, R.A., Hord, C., Horne, R.B., Jackson, D.R., Jones, B., Machin, S., Mitchell, C.N., Preston, J., Rees, J., Rogers, N.C., Routledge, G., Ryden, K., Tanner, R., Thomson, A.W.P., Wild, J.A. and Willis M. (2021) Development of Space Weather Reasonable Worst-Case Scenarios for the UK National Risk Assessment. *Space Weather*, **19**, e2020SW002593. https://doi.org/10.1029/2020SW002593

[3] Belisheva, N.K., Kanao, M., Kakinami, Y. and Toyokuni, G. (2019) The Effect of Space Weather on Human Body at the Spitsbergen Archipelago. IntechOpen, London. https://doi.org/10.5772/intechopen.85021

[4] Abdullrahman, H.M. and Marwa, A.M., (2020) The Effects of Solar Activity and Geomagnetic Disturbance on Human Health. *Open Access Journal of Biomedical Science*, **2**, 506-509. https://doi.org/10.38125/OAJBS.000203

[5] Yumi, N., Satoshi, N. and Atsuki, S. (2019) Relationship between the Low-Latitude Coronal Hole Area, Solar Wind Velocity and Geomagnetic Activity during Solar Cycles 23 and 24. *Planets and Space*, **71**, Article No. 24. https://doi.org/10.1186/s40623-019-1005-y

[6] Kusano, K., Ichimoto, K., Ishii, M., Miyoshi, Y., Yoden, S., Akiyoshi, H., *et al*. (2021) PSTEP: Project for Solar-Terrestrial Environment Prediction. *Earth*, *Planets and Space*, **73**, Article No. 159. https://doi.org/10.1186/s40623-021-01486-1

[7] Gnanou, I., Zoundi, C., Kaboré, S. and Ouattara, F. (2022) Variability of the Magnetospheric Electric Field Due to High-Speed Solar Wind Convection from 1964 to 2009. *African Journal of Environmental Science and Technology*, **16**, 1-9. https://doi.org/10.5897/AJEST2021.3075

[8] Wu, L., Gendrin, R., Higel, B. and Berchem, J. (1981) Relationships between the Solar Wind Electric Field and the Magnetospheric Convection Electric Field. *Geophysical Research Letters*, **8**, 1099-1102. https://doi.org/10.1029/GL008i010p01099

[9] Revah, I. and Bauer, P. (1982) Rapport d'activité du Centre de Recherches en Physique de l'environnement Terrestre et Planétaire, Note technique CRPE/115, 38-40 Rue du Général Leclerc 92131 Issy-Les Moulineaux.

[10] Wang, C., Han, J.P., Li, H., Peng, Z. and Richardson, J.D. (2014) Solar Wind-Magnetosphere Energy Coupling Function Fitting: Results from a Global MHD Simulation. *Journal of Geophysical Research*: *Space Physics*, **119**, 6199-6212. https://doi.org/10.1002/2014JA019834

[11] Milan, S.E., Gosling, J.S. and Hubert, B. (2012) Relationship between Interplanetary Parameters and the Magnetopause Reconnection Rate Quantified from Observations of the Expanding Polar Cap. *Journal of Geophysical Research: Space Physics*, **117**, n/a-n/a. https://doi.org/10.1029/2011JA017082

[12] Richardson Ian, G. and Hilary, V.C. (2012) Solar Wind Drivers of Geomagnetic Storms during More than Four Solar Cycles. *Journal of Space Weather and Space Climate*, **2**, Article No. A01. https://doi.org/10.1051/swsc/2012001

[13] Zerbo, J.-L., Amory-Mazaudier, C., Ouattara, F. and Richardson, J.D. (2012) Solar Wind and Geomagnetism: Toward a Standard Classification of Geomagnetic Activity from 1868 to 2009. *Annales Geophysicae*, **30**, 421-426. https://doi.org/10.5194/angeo-30-421-2012

[14] Mursula, K., Lukianova, R. and Holappa, L. (2015) Occurrence of High-Speed Solar Wind Streams over the Grand Modern Maximum. *The Astrophysical Journal*, **801**, Article No. 30. https://doi.org/10.1088/0004-637X/801/1/30

[15] Zerbo, J.-L., Amory-Mazaudier, C. and Ouattara, F. (2013) Geomagnetism during

Solar Cycle 23: Characteristics. *Journal of Advanced Research*, **4**, 265-274. https://doi.org/10.1016/j.jare.2012.08.010

[16] Poletto, G. (2013) Sources of Solar Wind over the Solar Activity Cycle. *Journal of Advanced Research*, **4**, 215-220. https://doi.org/10.1016/j.jare.2012.08.007

[17] Tsurutani, B.T., Gonzalez, W.D., Gonzalez, A.L.C., Tang, F., Arballo, J.K. and Okada, M. (1995) Interplanetary Origin of Geomagnetic Activity in the Declining Phase of the Solar Cycle. *Journal of Geophysical Research*: *Space Physics*, **100**, 21717-21733. https://doi.org/10.1029/95JA01476

[18] Echer, E., Alves, M.V. and Gonzalez, W.D. (2005) A Statistical Study of Magnetic Cloud Parameters and Geoeffectiveness. *Journal of Atmospheric and Solar-Terrestrial Physics*, **67**, 839-852. https://doi.org/10.1016/j.jastp.2005.02.010

[19] Maris, O. and Maris, G. (2005) Specific Features of the High-Speed Plasma Stream Cycles. *Advances in Space Research*, **35**, 2129-2140. https://doi.org/10.1016/j.asr.2005.02.068

[20] Tanskanen, E.I., Slavin, J.A., Tanskanen, A.J., Viljanen, A., Pulkkinen, T.I., Koskinen, H.E.J., Pulkkinen, A. and Eastwood, J. (2005) Magnetospheric Substorms Are Strongly Modulated by Interplanetary High-Speed Streams. *Geophysical Research Letters*, **32**, n/a-n/a. https://doi.org/10.1029/2005GL023318

[21] Kaboré, S. and Ouattara, F. (2018) Magnetosphere Convection Electric Field (MCEF) Time Variation from 1964 to 2009: Investigation on the Signatures of the Geoeffectiveness Coronal Mass Ejections. *International Journal of Physical Sciences*, **13**, 273-281. https://doi.org/10.5897/IJPS2018.4759

[22] Legrand, J.P. and Simon, P.A. (1989) Solar Cycle and Geomagnetic Activity: A Review for Geophysicists. Part I. The Contributions to Geomagnetic Activity of Shock Waves and of the Solar Wind. *Annales Geophysicae*, **7**, 565-578.

[23] Ouattara, F. and Amory-Mazaudier, C. (2009) Solar-Geomagnetic Activity and Aa Indices Toward a Standard Classification. *Journal of Atmospheric and Solar-Terrestrial Physics*, **71**, 1736-1748. https://doi.org/10.1016/j.jastp.2008.05.001

[24] Reeves, G.D., Morley, S.K., Friedel, R.H.W., Henderson, M.G., Cayton, T.E., Cunningham, G., Blake, B., Christensen, A.R. and Thomsen, D. (2011) On the Relationship between Relativistic Electron Flux and Solar Wind Velocity: Paulikas and Blake revisited. *Journal of Geophysical Research: Space Physics*, **116**, n/a-n/a. https://doi.org/10.1029/2010JA015735

[25] Obridko, V.N., Kanonidi, K.D., Mitrofanova, T.A. and Shelting, B.D. (2013) Solar Activity and Geomagnetic Disturbances. *Geomagnetism and Aeronomy*, **53**, 147-156. https://doi.org/10.1134/S0016793213010143

[26] Hajra, R., Tsurutani, B.T., Echer, E. and Gonzalez, W.D. (2014) Relativistic Electron Acceleration during High-Intensity, Long-Duration, Continuous *AE* Activity (HILDCAA) Events: Solar Cycle Phase Dependences. *Geophysical Research Letters*, **41**, 1876-1881. https://doi.org/10.1002/2014GL059383

[27] Hajra, R., Tsurutani, B.T., Echer, E., Gonzalez, W.D. and Santolik, O. (2015) Relativistic (E > 0.6, > 2.0 and > 4.0 MeV) Electron Acceleration at Geosynchronous Orbit during High-Intensity, Long-Duration, Continuous ae Activity (hildcaa) Events. *The Astrophysical Journal*, **799**, Article No. 39. https://doi.org/10.1088/0004-637X/799/1/39

[28] Hajra, R., Tsurutani, B.T., Echer, E., Gonzalez, W.D., Brum, C.G.M., Vieira, L.E.A. and Santolik, O. (2015) Relativistic Electron Acceleration during HILDCAA Events: Are Precursor CIR Magnetic Storms Important? *Earth*, *Planets and Space*, **67**, Article No. 109. https://doi.org/10.1186/s40623-015-0280-5

[29] Tsurutani, B.T., Gonzalez, W.D., Guarnieri, F., Kamide, Y., Zhou, X. and Arballo, J.K. (2004) Are High-Intensity Long-Duration Continuous AE Activity (HILDCAA) Events Substorm Expansion Events? *Journal of Atmospheric and Solar-Terrestrial Physics*, **66**, 167-176. https://doi.org/10.1016/j.jastp.2003.08.015

[30] Tsurutani, B.T., Hajra, R., Tanimori, T., Takada, A., Remya, B., Mannucci, A.J., Lakhina, G.S., Kozyra, J.U., Shiokawa, K., Lee, L.C., Echer, E., Reddy, R.V. and Gonzalez, W.D. (2016) Heliospheric Plasma Sheet (HPS) Impingement on to the Magnetosphere as a Cause of Relativistic Electron Dropouts (REDs) via Coherent EMIC Wave Scattering with Possible Consequences for Climate Change Mechanisms. *Journal of Geophysical Research*: *Space Physics*, **121**, 10130-10156. https://doi.org/10.1002/2016JA022499

[31] McGregor, S.L., Hughes, W.J., Arge, C.N., Owens, M.J. and Odstrcil, D. (2011) The Distribution of Solar Wind Speeds during Solar Minimum: Calibration for Numerical Solar Wind Modeling Constraints on the Source of the Slow Solar Wind. *Journal of Geophysical Research*, **116**, n/a-n/a. https://doi.org/10.1029/2010JA015881

[32] Villarreal D'Angelo, C., Schneiter, M., Costa, A., Velázquez, P., Raga, A. and Esquivel, A. (2014) On the Sensitivity of Extrasolar Mass-Loss Rate Ranges: HD 209458b a Case Study. *Monthly Notices of the Royal Astronomical Society*, **438**, 1654-1662. https://doi.org/10.1093/mnras/stt2303

[33] Rotter, T., Veronig, A.M., Temmer, M. and Vršnak, B. (2015) Real-Time Solar Wind Prediction Based on SDO/AIA Coronal Hole Data. *Solar Physics*, **290**, 1355-1370. https://doi.org/10.1007/s11207-015-0680-5

[34] Lindblad, B.A. (1990) Coronal Sources of High-Speed Plasma Streams in the Solar Wind during the Declining Phase of Solar Cycle 20. *Astrophysics and Space Science*, **170**, 55-61. https://doi.org/10.1007/BF00652645

[35] Richardson, I.G., Cliver, E.W. and Cane, H.V. (2000) Sources of Geomagnetic Activity over the Solar Cycle: Relative Importance of Coronal Mass Ejections, High-Speed Streams and Slow Solar Wind. *Journal of Geophysical Research*, **105**, 18203-18213. https://doi.org/10.1029/1999JA000400

[36] Bharati, K., Amar, K., Durbha, S.R. and Gurbax, S.L. (2019) Diminishing Activity of Recent Solar Cycles (22-24) and Their Impact on Geospace. *Journal of Space Weather and Space Climate*, **9**, Article No. A1. https://doi.org/10.1051/swsc/2018048

[37] D'Amicis, R., Telloni, D. and Bruno, R. (2020) The Effect of Solar-Wind Turbulence on Magnetospheric Activity. *Frontiers in Physics*, **8**, Article 604857. https://doi.org/10.3389/fphy.2020.604857

[38] Borovsky, J.E. (2003) MHD Turbulence in the Earth's Plasma Sheet: Dynamics, Dissipation and Driving. *Journal of Geophysical Research*, **108**, n/a-n/a. https://doi.org/10.1029/2002JA009625

[39] Osmane, A., Dimmock, A.P., Naderpour, R., Pulkkinen, T.I. and Nykyri, K. (2015) The Impact of Solar Wind ULF B_z Fluctuations on Geomagnetic Activity for Viscous Timescales during Strongly Northward and Southward IMF. *Journal of Geophysical Research*: *Space Physics*, **120**, 9307-9322. https://doi.org/10.1002/2015JA021505

[40] Sergeev, V.A., Pellinen, R.J. and Pulkkinen, T.I. (1996) Steady Magnetospheric Convection: A Review of Recent Results. *Space Science Reviews*, **75**, 551-604. https://doi.org/10.1007/BF00833344

[41] Milan, S.E., Carter, J.A., Sangha, H., Bower, G.E. and Anderson, B.J. (2021) Magnetospheric Flux Throughput in the Dungey Cycle: Identification of Convection State

during 2010. *Journal of Geophysical Research*: *Space Physics*, **126**, e2020JA028437. https://doi.org/10.1029/2020JA028437

[42] Chang, T. (1992) Low-Dimensional Behavior and Symmetry-Breaking of Stochastic Systems Near Criticality Can These Effects Be Observed in Space and in the Laboratory? *IEEE Transactions on Plasma Science*, **20**, 691-694. https://doi.org/10.1109/27.199515

[43] Klimas, A.J., Vassiliadis, D., Baker, D.N. and Roberts, D.A. (1996) The Organized Nonlinear Dynamics of the Magnetosphere. *Journal of Geophysical Research*: *Space Physics*, **101**, 13089-130113. https://doi.org/10.1029/96JA00563

[44] Consolini, G. (2002) Self-Organized Criticality: A New Paradigm for the Magnetotail Dynamics. *Fractals*, **10**, 275-283. https://doi.org/10.1142/S0218348X02001397

[45] Valdivia, J., Rogan, J., Munoz, V., Gomberoff, L., Klimas, A., Vassiliadis, D., Uritsky, V., Sharma, S., Toledo, B. and Wastavino, L. (2005) The Magnetosphere as a Complex System. *Advances in Space Research*, **35**, 961-971. https://doi.org/10.1016/j.asr.2005.03.144

[46] Watkins, N.W., Freeman, M.P., Chapman, S.C. and Dendy, R.O. (2011) Testing the Soc Hypothesis for the Magnetosphere. *Journal of Atmospheric and Solar-Terrestrial Physics*, **63**, 1435-1445. https://doi.org/10.1016/S1364-6826(00)00245-5

[47] Pulkkinen, T.I., Goodrich, C.C. and Lyon, J.G. (2007) Solar Wind Electric Field Driving of Magnetospheric Activity: Is It Velocity or Magnetic Field? *Geophysical Research Letters*, **34**, n/a-n/a. https://doi.org/10.1029/2007GL031011

[48] Borovsky, J.E. and Denton, M.H. (2006) Effect of Plasmaspheric Drainage Plumes on Solar-Wind/Magnetosphere Coupling. *Geophysical Research Letters*, **33**, n/a-n/a. https://doi.org/10.1029/2006GL026519

[49] Denton, M.H. and Borovsky, J.E. (2008). Superposed Epoch Analysis of High-Speed-Stream Effects at Geosynchronous Orbit: Hot Plasma, Cold Plasma, and the Solar Wind. *Journal of Geophysical Research*: *Space Physics*, **113**, n/a-n/a. https://doi.org/10.1029/2007JA012998

[50] Borovsky, J.E. and Denton, M.H. (2009). Relativistic-Electron Dropouts and Recovery: A Superposed Epoch Study of the Magnetosphere and the Solar Wind. *Journal of Geophysical Research*: *Space Physics*, **114**, n/a-n/a. https://doi.org/10.1029/2008JA013128

[51] Reistad, J.P., Holappa, L., Ohma, A., Gabrielse, C., Sur, D., Asikainen, T. and De Jong, A. (2022) Dependence of the Global Dayside Reconnection Rate on Interplanetary Magnetic Field B_y and the Earth's Dipole Tilt. *Frontiers in Astronomy and Space Sciences*, **9**, Article 973276. https://doi.org/10.3389/fspas.2022.973276

[52] Dungey, J.W. (1961) Interplanetary Magnetic Field and the Auroral Zones. *Physical Review Letters*, **6**, 47-48. https://doi.org/10.1103/PhysRevLett.6.47

[53] Marchaudon, A., Blelly, P.-L., Grandin, M., Aikio, A., Kozlovsky, A. and Virtanen, I. (2018) IPIM Modeling of the Ionospheric F_2 Layer Depletion at High-Latitudes during a High-Speed Stream Event. *Journal of Geophysical Research*: *Space Physics*, **123**, 7051-7066. https://doi.org/10.1029/2018JA025744

[54] Milan, S.E., Boakes, P.D. and Hubert, B. (2008) Response of the Expanding/Contracting Polar Cap to Weak and Strong Solar Wind Driving: Implications for Substorm Onset. *Journal of Geophysical Research*: *Space Physics*, **113**, n/a-n/a. https://doi.org/10.1029/2008JA013340

[55] Ohma, A., Reistad, J.P. and Hatch, S.M. (2021) Modulation of Magnetospheric Substorm Frequency: Dipole Tilt and IMF B_y Effects. *Journal of Geophysical Research*: *Space Physics*, **126**, e2020JA028856. https://doi.org/10.1029/2020JA028856

[56] Funke, B., López-Puertas, M., Gil-López, S., Von Clarmann, T., Stiller, G.P., Fischer, H. and Kellmann, S. (2005) Downward transport of upper atmospheric NOx into the polar stratosphere and lower mesosphere during the Antarctic 2003 and Arctic 2002/2003 Winters. *Journal of Geophysical Research*: *Atmospheres*, **110**, n/a-n/a. https://doi.org/10.1029/2005JD006463

[57] Randall, C.E., Harvey, V.L., Singleton, C.S., Bailey, S.M., Bernath, P.F., Codrescu, M., Nakajima, H. and Russell, J.M. (2007) Energetic particle precipitation effects on the Southern Hemisphere stratosphere in 1992-2005. *Journal of Geophysical Research*, **112**, n/a-n/a. https://doi.org/10.1029/2006JD007696

[58] Seppälä, A., Verronen, P.T., Clilverd, M.A., Randall, C.E., Tamminen, J., Sofieva, V., Backman, L. and Kyrölä, E. (2007) Arctic and Antarctic polar winter NOxand energetic particle precipitation in 2002-2006. *Geophysical Research Letters*, **34**, n/a-n/a. https://doi.org/10.1029/2007GL029733